LETTERS TO THE EDITOR

This Letters section is for publishing (a) brief acoustical research or applied acoustical reports, (b) comments on articles or letters previously published in this Journal, and (c) a reply by the article author to criticism by the Letter author in (b). Extensive reports should be submitted as articles, not in a letter series. Letters are peer-reviewed on the same basis as articles, but usually require less review time before acceptance. Letters cannot exceed four printed pages (approximately 3000–4000 words) including figures, tables, references, and a required abstract of about 100 words.

The diffracted field and its gradient near the edge of a thin screen (L)

David P. Hewett[a)]
Department of Mathematics and Statistics, University of Reading, Whiteknights, P.O. Box 220, Reading, RG6 6AX, United Kingdom

U. Peter Svensson
Acoustics Research Centre, Department of Electronics and Telecommunications, Norwegian University of Science and Technology, NO-7491 Trondheim, Norway

(Received 24 May 2013; revised 19 August 2013; accepted 15 October 2013)

The secondary edge source line integral formulation for diffraction modeling uses edge sources with a $1/r$ dependency, in addition to a directivity function. At first sight, this might seem to contradict the expected $1/\sqrt{r}$ behavior for the gradient near the edge of a thin screen. An analysis is presented for the special case of perpendicular plane wave incidence onto a thin screen, which shows that the secondary edge source formulation does indeed lead to the expected behavior close to the edge of an ideal wedge.
 [http://dx.doi.org/10.1121/1.4828824]

PACS number(s): 43.20.El, 43.20.Fn [JES] Pages: 4303–4306

I. INTRODUCTION

Edge diffraction formulations have proven to be very useful in scattering studies. A recent integral equation formulation, which permits the computation of arbitrarily high orders of diffraction, has been shown to give consistent results down to 0 Hz for convex, rigid scatterers.[1] Low orders of diffraction have been employed also in highly complex geometries, using a time-domain formulation.[2] Also, comparisons between the boundary element method and an edge diffraction based formulation indicate the efficiency of the latter approach for outdoor sound propagation studies.[3]

The field diffracted by an infinite wedge of arbitrary wedge angle, under point source excitation, is known to have a number of equivalent exact closed-form representations. Frequency-domain expressions include line integral formulations and infinite series expansions,[4–6] and time-domain expressions are also available in explicit forms,[7] referred to here as the BT-solution. Equivalently, these solutions can be expressed in a more physically intuitive form as a line integral over contributions due to directional secondary edge sources, for both the time-domain[8] and frequency-domain[9] cases.

In representing the solution for the wedge diffraction problem it is natural to decompose the total sound field into three components: The direct field, the specularly reflected field (depending on the geometry, zero, one, or more specular reflections might exist), and the remaining diffracted field. The first two components are non-zero only in certain regions of the physical domain: The direct field is non-zero only for receiver positions with a direct line-of-sight to the source, and the specularly reflected field is non-zero only in regions where the receiver can "see" the relevant image source(s). The resulting discontinuities in these two components across the boundaries of the associated regions in which they are non-zero (i.e., across the shadow zone boundaries) necessarily make the last component, the diffracted field, discontinuous as well.

These discontinuities in the diffracted field across the shadow zone boundaries have been analyzed and described both for the traditional frequency-domain expressions and for the time-domain BT solution.[10,11] Obviously, the secondary edge source line integral formulation must possess the same characteristics around shadow zone boundaries, and this has been verified in Ref. 12.

The aim of this note is to verify that the secondary edge source formulation also possesses the correct near-edge behavior for the field and its gradient, both for the Neumann boundary condition and for the Dirichlet boundary condition. For simplicity the analysis will be limited to plane wave incidence on a thin screen (with exterior wedge angle $\theta_W = 2\pi$).

II. THE SECONDARY EDGE SOURCE LINE INTEGRAL

The diffracted field from an infinite edge, as caused by a monopole source, can be written as a line integral over contributions by secondary edge sources,

$$p_d = -\frac{\nu}{4\pi}\int_{-\infty}^{\infty} \frac{e^{-jk(m+l)}}{ml}\beta dz, \tag{1}$$

[a)]Author to whom correspondence should be addressed. Current address: Mathematical Institute, University of Oxford, Radcliffe Observatory Quarter, Woodstock Road, Oxford, OX2 6GG, United Kingdom. Electronic mail: hewett@maths.ox.ac.uk

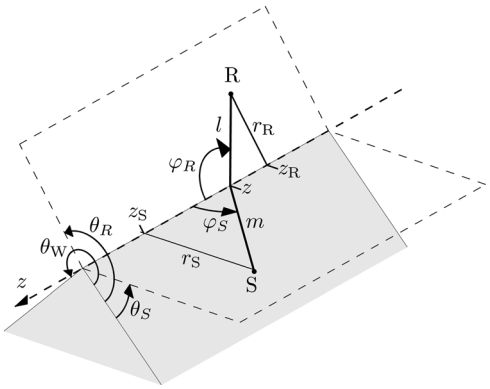

FIG. 1. The geometry of the wedge.

where $\nu = \pi/\theta_W$ is the wedge index (θ_W being the exterior wedge angle), z is a position along the edge, and m and l are distances from the edge point z to the source and receiver, respectively,[9] as illustrated in Fig. 1. Furthermore, the factor β, which can be interpreted as a directivity function, has the following forms for the Neumann and Dirichlet boundary conditions, respectively (in both cases, both wedge faces have the same boundary condition),

$$\beta^{\mathrm{N}} = \beta_1 + \beta_2 + \beta_3 + \beta_4, \quad \beta^{\mathrm{D}} = \beta_1 - \beta_2 - \beta_3 + \beta_4,$$

where

$$\beta_i = \frac{\sin(\nu\varphi_i)}{\cosh(\nu\eta) - \cos(\nu\varphi_i)},$$

the angles φ_i are

$$\varphi_1 = \pi + \theta_S + \theta_R, \quad \varphi_2 = \pi + \theta_S - \theta_R,$$
$$\varphi_3 = \pi - \theta_S + \theta_R, \quad \varphi_4 = \pi - \theta_S - \theta_R,$$

and the auxiliary function η is

$$\eta = \cosh^{-1}\frac{(z - z_S)(z - z_R) + ml}{r_S r_R}, \tag{2}$$

with $0 \le \theta_S, \theta_R \le 2\pi$ and $r_S, r_R \ge 0$ denoting the source and receiver positions in cylindrical polar coordinates centered on the edge. [Note that Eq. (2) corrects a sign error in the corresponding formula in Ref. 9.] The function η can also be written in terms of local in-plane angles around the edge point z which therefore motivates why the β factors can be called directivity functions,

$$\eta = \cosh^{-1}\frac{1 + \cos\varphi_S \cos\varphi_R}{\sin\varphi_S \sin\varphi_R},$$

where φ_S is the angle between the edge, in the positive z-direction, and the line from the edge point z to the source. Similarly, φ_R is the angle between the edge, in the positive z-direction, and the line from the edge point z to the receiver, see Fig. 1.

Since the only θ_R-dependence in Eq. (1) is in β,

$$\frac{\partial p_d}{\partial \theta_R} = -\frac{\nu}{4\pi}\int_{-\infty}^{\infty} \frac{\mathrm{e}^{-jk(m+l)}}{ml}\frac{\partial \beta}{\partial \theta_R}dz. \tag{3}$$

From this one can compute the field gradient normal to the two wedge surfaces $\theta = 0$ and $\theta = \theta_W$ as

$$\frac{\partial p_d}{\partial n} = \frac{\partial p_d}{\partial \theta_R}\frac{\partial \theta_R}{\partial n}\bigg|_{\substack{\theta_R = 0 \\ \text{or } \theta_R = \theta_W}} = \pm\frac{1}{r_R}\frac{\partial p_d}{\partial \theta_R}\bigg|_{\substack{\theta_R = 0 \\ \text{or } \theta_{R=}\theta_W}}, \tag{4}$$

where n is assumed to point into the physical domain and the upper (+) and lower (−) signs are required for $\theta_R = 0$ and $\theta_R = \theta_W$, respectively.

That Eq. (1) satisfies the correct boundary conditions on the wedge surfaces in the Dirichlet and Neumann cases, respectively, is easily verified by noting that β^D and $\partial\beta^N/\partial\theta_R$ both vanish for $\theta_R = 0$ and $\theta_R = \theta_W$.

A. Plane wave incidence perpendicular to the edge

For the special but important case of plane wave incidence perpendicular to the edge, the source and receiver are placed at $z_S = z_R = 0$, and $\varphi_S = \pi/2$ (recall Fig. 1), so that

$$\cosh(\nu\eta)^{\mathrm{PW}} = \cosh\left(\nu\cosh^{-1}\frac{1}{\sin\varphi_R}\right). \tag{5}$$

Because of symmetry, the integration range in Eqs. (1) and (3) can be halved. Furthermore, plane wave incidence implies that the $1/m$ spherical attenuation factor should be removed, and if one chooses to refer the phase of the diffracted sound pressure relative to the arrival time at the edge, the phase oscillation factor e^{-jkm} also disappears. In this case one obtains, with $l = \sqrt{r_R^2 + z^2}$,

$$p_d^{\mathrm{PW}} = -\frac{\nu}{2\pi}\int_0^{\infty}\frac{\mathrm{e}^{-jkl}}{l}\beta dz, \tag{6}$$

$$\frac{\partial p_d^{\mathrm{PW}}}{\partial \theta_R} = -\frac{\nu}{2\pi}\int_0^{\infty}\frac{\mathrm{e}^{-jkl}}{l}\frac{\partial \beta}{\partial \theta_R}dz. \tag{7}$$

In the case of a thin screen, for which $\theta_W = 2\pi$ and $\nu = 1/2$, further simplification is obtained. In particular, Eq. (5) becomes

$$\cosh\left(\frac{\eta}{2}\right)^{\mathrm{PW}} = \frac{1}{\sqrt{2}}\sqrt{1 + \frac{l}{r_R}} = \frac{1}{\sqrt{2}}\sqrt{1 + \sqrt{1 + \frac{z^2}{r_R^2}}}. \tag{8}$$

III. THE FIELD NEAR THE EDGE OF THE THIN NEUMANN SCREEN

The field near the edge of a thin Neumann screen ($\nu = 1/2$) is expected to have a finite limit value. This will be verified below for two specific cases of plane wave incidence perpendicular to the edge: First perpendicular to the screen ($\theta_S = \pi/2$), and then along the screen ($\theta_S = 0$). In both cases the receiver will lie on the screen, i.e., with $\theta_R = 0$ or $\theta_R = 2\pi$.

A. Incidence perpendicular to the screen ($\theta_S = \pi/2$)

For $\theta_S = \pi/2$ and $\theta_R = 0$ or $\theta_R = \theta_W$, β simplifies to

$$\beta^{\mathrm{N,PW}}_{\theta_S = \pi/2} = \pm 4\frac{r_R}{l}\sqrt{1 + \frac{l}{r_R}}, \tag{9}$$

where, as above, the upper (+) and lower (−) signs are required for $\theta_R = 0$ and $\theta_R = \theta_W$, respectively. When inserted in Eq. (6), with $\nu = 1/2$, this gives

$$p_d^{\mathrm{N,PW}} = \mp\frac{1}{\pi}\int_0^\infty \frac{r_R \mathrm{e}^{-jkl}}{l^2}\sqrt{1+\frac{l}{r_R}}dz, \tag{10}$$

which, by the change of variable $z = r_R t$, can be written

$$p_d^{\mathrm{N,PW}} = \mp\frac{1}{\pi}\int_0^\infty \frac{\mathrm{e}^{-jkr_R\sqrt{1+t^2}}\sqrt{1+\sqrt{1+t^2}}}{1+t^2}dt.$$

As $kr_R \to 0$ this tends to the finite limit

$$p_d^{\mathrm{N,PW}} \sim \mp\frac{1}{\pi}\int_0^\infty \frac{\sqrt{1+\sqrt{1+t^2}}}{1+t^2}dt.$$

The integral in this expression can be evaluated in closed form, e.g., by using a further change of variables $v = \sqrt{1+t^2}-1$ to obtain the integral

$$\int_0^\infty \frac{1}{(v+1)\sqrt{v}}dv = \pi,$$

so that

$$p_d^{N,PW} \to \mp 1, \quad kr_R \to 0.$$

These limiting values are as expected: The direct and specularly reflected fields sum to give the geometrical acoustics approximations $p_{\mathrm{GA}} = 2$ and $p_{\mathrm{GA}} = 0$ on the illuminated side ($\theta_R = 0$) and the shadow side ($\theta_R = 2\pi$), respectively, but near the edge (on either side) the total field should be $p_{\mathrm{tot}} = 1$, which is fulfilled by a diffracted field of amplitude ∓ 1, respectively.

B. Incidence along the screen ($\theta_S = 0$)

For $\theta_S = 0$ and $\theta_R = 0$ or $\theta_R = \theta_W$, β again has a simple expression,

$$\beta_{\theta_S=0}^{\mathrm{N,PW}} = \pm\frac{4}{\cosh\frac{\eta}{2}} = \frac{4\sqrt{2}}{\sqrt{1+\frac{l}{r_R}}}, \tag{11}$$

with the same sign convention as above. When inserted in Eq. (6), with $\nu = 1/2$, this gives

$$p_d^{\mathrm{N,PW}} = -\frac{\sqrt{2}}{\pi}\int_0^\infty \frac{\mathrm{e}^{-jkl}}{l\sqrt{1+\frac{l}{r_R}}}dz, \tag{12}$$

and, after the change of variable $z = r_R t$, one obtains

$$p_d^{\mathrm{N,PW}} = -\frac{\sqrt{2}}{\pi}\int_0^\infty \frac{\mathrm{e}^{-jkr_R\sqrt{1+t^2}}}{\sqrt{1+t^2}\sqrt{1+\sqrt{1+t^2}}}dt.$$

As $kr_R \to 0$ this tends to a finite limit

$$p_d^{\mathrm{N,PW}} \sim \mp\frac{\sqrt{2}}{\pi}\int_0^\infty \frac{1}{\sqrt{1+t^2}\sqrt{1+\sqrt{1+t^2}}}dt.$$

The same change of variables $v = \sqrt{1+t^2}-1$ used above allows the integral in this expression to be evaluated as

$$\int_0^\infty \frac{1}{(v+2)\sqrt{v}}dv = \frac{\pi}{\sqrt{2}},$$

so that once again, as expected,

$$p_d^{N,PW} \to \mp 1, \quad kr_R \to 0.$$

IV. THE GRADIENT OF THE FIELD NEAR THE EDGE OF THE THIN NEUMANN SCREEN

The gradient of the field is expected to be singular at the edge. To investigate this, the behavior of the gradient across the extension of the screen (i.e., $\theta_R = \pi$) is considered, in the limit as the edge is approached. For brevity only incidence perpendicular to the screen ($\theta_S = \pi/2$) is considered.

First note that, for $\theta_S = \pi/2$ and $\theta_R = \pi$,

$$\left.\frac{\partial\beta^{\mathrm{N,PW}}}{\partial\theta_R}\right|_{\substack{\theta_S=\pi/2\\ \theta_R=\pi}} = -2\left(\frac{r_R}{l}\right)^2\sqrt{1+\frac{l}{r_R}}\left(2-\frac{l}{r_R}\right). \tag{13}$$

Then, if $\tilde{n}$ is the normal vector to the line $\theta_R = \pi$ pointing in the direction of increasing θ_R, it holds by Eq. (7) that

$$\frac{\partial p_d^{\mathrm{N,PW}}}{\partial\tilde{n}} = \frac{1}{r_R}\left.\frac{\partial p_d}{\partial\theta_R}\right|_{\substack{\theta_S=\pi/2\\ \theta_R=\pi}} = \frac{1}{2\pi r_R}I, \tag{14}$$

where

$$I = \int_0^\infty \mathrm{e}^{-jkr_R\sqrt{1+t^2}}\frac{\sqrt{1+\sqrt{1+t^2}}}{(1+t^2)^{3/2}}\left(\sqrt{1+t^2}-2\right)dt.$$

The further change of variable $v = \sqrt{1+t^2}-1$ gives

$$I = \mathrm{e}^{-jkr_R}\int_0^\infty \frac{\mathrm{e}^{-jkr_R v}(v-1)}{(v+1)^2\sqrt{v}}dv. \tag{15}$$

Setting $kr_R = 0$ in Eq. (15) gives a convergent integral,

$$I|_{kr_R=0} = \int_0^\infty \frac{(v-1)}{(v+1)^2\sqrt{v}}dv < \infty, \tag{16}$$

which, recalling Eq. (14), might at first suggest that the field gradient blows up like $1/r_R$ as the edge is approached, in contradiction to the inverse square root singularity observed in other solution representations.[5] However, this apparent discrepancy is an illusion, because the integral in Eq. (16) is in fact equal to zero. This is easily checked by noting, using a change of variable $v = 1/w$, that

$$\int_0^\infty \frac{\sqrt{v}}{(v+1)^2}dv = \int_0^\infty \frac{1}{(w+1)^2\sqrt{w}}dw.$$

The correct singular behavior can be recovered by a more careful asymptotic approximation of Eq. (15) in the limit as $kr_R \to 0$, as will now be demonstrated.

First, for notational convenience, set $\epsilon := kr_R$, so that

$$I = \mathrm{e}^{-j\epsilon}\int_0^\infty \frac{(v-1)\,\mathrm{e}^{-j\epsilon v}}{(v+1)^2\sqrt{v}}dv.$$

Then, splitting the integration range at $v = v_*$, for some $1 \ll v_* \ll 1/\epsilon = 1/(kr_R)$ (to be specified later) and expanding the exponential and algebraic factors in the integrand into their respective asymptotic series (where this is valid) gives, as $\epsilon \to 0$,

$$
\begin{aligned}
\mathrm{e}^{j\epsilon} I &\sim \int_0^{v_*} \frac{(v-1)}{(v+1)^2\sqrt{v}}(1 - j\epsilon v + \cdots)\, dv \\
&\quad + \int_{v_*}^{\infty} \frac{\mathrm{e}^{-j\epsilon v}}{\sqrt{v}}\left(\frac{1}{v} - \frac{3}{v^2} + \cdots\right) dv \\
&\sim \int_0^{v_*} \frac{(v-1)}{(v+1)^2\sqrt{v}} dv - j\epsilon \int_0^{v_*} \frac{(v-1)\sqrt{v}}{(v+1)^2} dv + \cdots \\
&\quad + \int_{v_*}^{\infty} \frac{\mathrm{e}^{-j\epsilon v}}{v^{3/2}} dv - 3\int_{v_*}^{\infty} \frac{\mathrm{e}^{-j\epsilon v}}{v^{5/2}} dv + \cdots . \qquad (17)
\end{aligned}
$$

The first and second integrals on the right-hand side of Eq. (17) can be evaluated in closed form, and satisfy (recall $v_* \gg 1$)

$$
\begin{aligned}
&\int_0^{v_*} \frac{(v-1)}{(v+1)^2\sqrt{v}} dv \sim -\frac{2}{\sqrt{v_*}} + \mathcal{O}\left(\frac{1}{v_*^{3/2}}\right), \\
&-j\epsilon \int_0^{v_*} \frac{(v-1)\sqrt{v}}{(v+1)^2} dv \sim -j\epsilon(2\sqrt{v_*} + \mathcal{O}(1)).
\end{aligned}
$$

The third integral can be estimated using integration by parts, and satisfies (recall $\epsilon v_* \ll 1$)

$$
\int_{v_*}^{\infty} \frac{\mathrm{e}^{-j\epsilon v}}{v^{3/2}} dv \sim \sqrt{\epsilon}\left(\frac{2}{\sqrt{\epsilon v_*}} + 2\sqrt{\pi}\mathrm{e}^{-j3\pi/4} + \mathcal{O}(\sqrt{\epsilon v_*})\right),
$$

while the fourth integral is easily estimated, with

$$
-3\int_{v_*}^{\infty} \frac{\mathrm{e}^{-j\epsilon v}}{v^{5/2}} dv = \mathcal{O}\left(\frac{1}{v_*^{3/2}}\right).
$$

Inserting these estimates in Eq. (17), taking $v_* = 1/\sqrt{\epsilon}$, and collecting like powers of ϵ, one finds that the leading order terms arising from the first and third integrals cancel, yielding the estimate

$$
I \sim 2\sqrt{\pi}\mathrm{e}^{-j3\pi/4}\sqrt{\epsilon}, \quad \epsilon \to 0.
$$

Consequently, recalling Eq. (14), the expected singular behavior[5] is obtained, namely,

$$
\frac{\partial p_d^{\mathrm{N,PW}}}{\partial \tilde{n}} \sim \sqrt{\frac{k}{\pi r_R}}\mathrm{e}^{-j3\pi/4}, \quad kr_R \to 0.
$$

V. THE GRADIENT OF THE FIELD NEAR THE EDGE OF THE THIN DIRICHLET SCREEN

For the Dirichlet case, the diffracted field is zero on the screen, but the normal derivative of the field is expected to have an inverse square root singularity. Again, for brevity only the case of plane wave incidence normal to the screen ($\theta_S = \pi/2$) is considered. In this case, with $\theta_R = 0$ or $\theta_R = 2\pi$ one finds that

$$
\left.\frac{\beta^{\mathrm{D,PW}}}{\partial n}\right|_{\substack{\theta_S = \pi/2 \\ \theta_R = 0 \text{ or } \theta_R = 2\pi}} = \mp 2\left(\frac{r_R}{l}\right)^2 \sqrt{1 + \frac{l}{r_R}}\left(2 - \frac{l}{r_R}\right),
$$

where, as usual, the upper and lower signs are required for $\theta_R = 0$ and $\theta_R = 2\pi$, respectively. Hence, recalling Eqs. (4) and (7) one finds that the normal derivative on either side of the screen is given by

$$
\left.\frac{\partial p_d^{\mathrm{D,PW}}}{\partial n}\right|_{\theta_R = 0} = \left.\frac{\partial p_d^{\mathrm{D,PW}}}{\partial n}\right|_{\theta_R = 2\pi} = -\frac{1}{2\pi r_R} I,
$$

where I is defined exactly as in Sec. IV. Thus it is clear that as $kr_R \to 0$,

$$
\left.\frac{\partial p_d^{\mathrm{D,PW}}}{\partial n}\right|_{\theta_R = 0} = \left.\frac{\partial p_d^{\mathrm{D,PW}}}{\partial n}\right|_{\theta_R = 2\pi} \sim -\sqrt{\frac{k}{\pi r_R}}\mathrm{e}^{-j3\pi/4},
$$

and this corresponds to the known behavior.[5]

VI. CONCLUSIONS

The secondary edge source line integral for diffraction modeling has been analyzed with respect to the singular behavior near the edge of a thin screen, for the special case of plane wave incidence perpendicular to the edge. The analysis shows that the diffracted field at the edge of a Neumann screen has the limit value -1 in the illuminated zone, and $+1$ in the shadow zone. The field gradient for the Neumann screen has the expected $1/\sqrt{r}$ behavior near the edge in spite of the apparent $1/r$-factor in the line integral. Similarly, the field gradient normal to a Dirichlet screen also has the correct $1/\sqrt{r}$ singularity. A similar analysis should also be possible for wedges with exterior angles other than $\theta_W = 2\pi$, starting from the general expressions in Eqs. (6) and (7), but we expect the details to be more complicated, and we leave this for further studies.

ACKNOWLEDGMENT

The authors gratefully acknowledge helpful discussions with S. N. Chandler-Wilde (University of Reading, United Kingdom) during the preparation of this paper.

[1] A. Asheim and U. P. Svensson, "An integral equation formulation for the diffraction from convex plates and polyhedra," J. Acoust. Soc. Am. **133**, 3681–3691 (2013).

[2] L. Antani, A. Chandak, M. Taylor, and D. Manocha, "Efficient finite-edge diffraction using conservative from-region visibility," Appl. Acoust. **73**(3), 218–233 (2012).

[3] M. C. Remillieux, J. M. Corcoran, T. R. Haac, R. A. Burdisso, and U. P. Svensson, "Experimental and numerical study on the propagation of impulsive sound around buildings," Appl. Acoust. **73**(10), 1029–1044 (2012).

[4] T. M. Macdonald, "A class of diffraction problems," Proc. London Math. Soc. **14**, 410–427 (1915).

[5] J. J. Bowman and T. B. A. Senior, "Chapter 6: The wedge" in *Electromagnetic and Acoustic Scattering by Simple Shapes*, edited by J. J. Bowman, T. B. A. Senior, and P. L. E. Uslenghi (Hemisphere Publishing Corporation, New York, 1969), pp. 252–283.

[6] A. D. Pierce, *Acoustics: An Introduction to its Physical Principles and Applications* (The Acoustical Society of America, Woodbury, NY, 1989), pp. 481–494.

[7] M. A. Biot and I. Tolstoy, "Formulation of wave propagation in infinite media by normal coordinates with an application to diffraction," J. Acoust. Soc. Am. **29**, 381–391 (1957).

[8] U. P. Svensson, R. I. Fred, and J. Vanderkooy, "An analytic secondary source model of edge diffraction impulse responses," J. Acoust. Soc. Am. **106**, 2331–2344 (1999).

[9] U. P. Svensson, P. T. Calamia, and S. Nakanishi, "Frequency-domain edge diffraction for finite and infinite edges," Acta Acust. Acust. **95**, 568–572 (2009).

[10] W. A. Kinney, C. S. Clay, and G. A. Sandness, "Scattering from a corrugated surface: Comparison between experiment, Helmholtz-Kirchhoff theory, and the facet-ensemble method," J. Acoust. Soc. Am. **73**, 183–194 (1983).

[11] D. Ouis, "Diffraction by a hard half-plane: useful approximations to an exact formulation," J. Sound Vib. **252**, 191–221 (2002).

[12] U. P. Svensson and P. T. Calamia, "Edge-diffraction impulse responses near specular-zone and shadow-zone boundaries," Acta Acust. Acust. **92**, 501–512 (2006).